

1 **The role of Gut Microbiome in Anorexia Nervosa**

2

3 Manuela O Deigh, Nia Walker, Safa Malik

4

5 Department of Bioinformatics and Computational Biology, University of Maryland,
6 College Park, MD

7

8 One sentence description

9 Gut microbiome alterations modulate hypothalamic gene expression and microbial
10 diversity in mouse models of anorexia, providing insights into neuropeptide regulation
11 mechanisms.

12

13 Key words

14 Gut microbiome, Eating disorders, Activity-based anorexia model, Appetite regulation,
15 Neuropeptide Y, Gut barrier

16

17 **ABSTRACT**

18 The gut microbiome has a profound impact on neuropsychiatric disorders and is
19 hypothesized to influence neuropeptides associated with appetite regulation and
20 perception. In this project, we aim to investigate the impact of microbiome alterations on
21 hypothalamic gene expression and microbial diversity. We perform bioinformatic
22 analyses on 16S rRNA sequencing data following an activity-based anorexia (ABA)
23 mouse model experiment [1] to explore microbial and gene expression changes in
24 antibiotic-treated, germ-free, and control mice. The associated experiment samples'
25 sequencing data were downloaded from the SRA (PRJEB70936) and processed on the
26 UMD bioi605 cluster using a reproducible DADA2- pipeline. This included quality score
27 assessment, trimming, dereplication, denoising, chimera removal, and taxonomic
28 assignment using the SILVA 138.2 database. This manuscript outlines the initial data
29 processing and analysis steps in preparation for downstream statistical and biological
30 interpretation.

31

32

33 **INTRODUCTION**

34 Anorexia nervosa (AN) is a complex psychiatric disorder marked by extreme food
35 restriction, low body weight, and an intense fear of gaining weight, often accompanied
36 by excessive exercise and a distorted body image. While traditionally viewed as a
37 behavioral condition, recent research highlights the potential role of systemic
38 inflammation and altered gut microbiota in its pathophysiology, as AN patients exhibit
39 signs of chronic low-grade inflammation, leading to deficits in intestinal permeability. [2]

40 Evidence suggests that the gut-brain axis, particularly microbiome-mediated modulation
41 of hypothalamic appetite regulation, may contribute to the onset and persistence of AN.
42 To explore this, this study uses a mouse model combining food restriction and
43 hyperactivity to investigate the influence of the gut microbiome (specifically the
44 expression levels of eight hypothalamic appetite-regulating peptides and two reference
45 genes) on the onset and progression of AN.

46 The research studies three groups of mice: control (healthy gut microbiome), antibiotic-
47 treated, and germ-free (with no microbiome). Mice were further divided based on diet
48 and access to a running wheel across three experimental phases.

49 The groups of mice are summarized in the table below:

	Fed ad libitum (AL)	Fed restrictively (FR)
Access to running wheel	Access, AL	Access, FR
No access to running wheel	No access, AL	No access, FR

50 Fecal samples from all the groups were collected at the end of each phase, genomic
51 DNA was isolated and used to construct bacterial 16S rRNA amplicon sequencing
52 libraries. As part of the gene expression analysis, six appetite-regulating neuropeptides,
53 two intestinal tight junction proteins and two mucin protein family members were
54 studied.

55 The supplementary table from the original study paper lists the primers studied.

56 Supplementary Table 1: List of primers used for gene expression analysis in mouse hypothalamus and intestine.

Gene	Forward Primer (5' → 3')	Reverse Primer (3' → 5')	Amplicon length (bp)
Hypothalamus			

<i>Actb</i>	TTGCTGACAGGATGCAGAAG	GTACTTGCCTCAGGAGGAG	86
<i>NPY</i>	CTGCGACACTACATCAATCT	CTTCAAGCCTGTTCTGG	124
<i>AgRP</i>	TGCAGACCGAGCAGAAGAAG	GACTCGTCAGCCTTACACA	114
<i>MCH</i>	AGCATCAAACTAAGGATGGCA	GGCGACAACGGATCTTCTG	195
<i>Orexin</i>	ACCGTAACTACCACCGCTT	GGGGGAAGTTGGATCAGGA	86
<i>CRH</i>	GAAAATGTGGCCCCAAGGAG	AGCCACCCCTCAAGAATGAA	106
<i>TRH</i>	TCTGCAGAGTCTCCACCTTG	CGAAGATCAAAGCCAGAGCC	73
<i>CART</i>	GCTGCTACTGCTACCTTGC	TTCGATCAGCTCCTCTCGT	118
<i>POMC</i>	CCATAGATGTGTGGAGCTGGTG	CATCTCCGTTGCCAGGAAACAC	365

Intestine

<i>Hprt</i>	GGTTAACGAGTACAGCCCCA	GGCCTGTATCCAACACTTCG	81
<i>CasC3</i>	TTCGAGGTGTGCCTAACCA	GCTTAGCTCGACCACTCTGG	96
<i>ZO-1</i>	CCACCTCTGTCCAGCTCTTC	CACCGGAGTGATGGTTTCT	249
<i>OCCLU</i>	actcctcaatggacAaagtg	ccccacacctgtcgtagtct	249b
<i>MUC2</i>	GATGGCACCTACCTCGTTGT	GTCCTGGCACTTGTGGAAT	246
<i>MUC13</i>	GAGGAGAAACAGGGAGCATAG	GGACATCAAGGGAGAAG	107

57 *Hprt* - Hypoxanthine phospho-ribosyltransferase 1; *ActB* - Actin beta; *NPY* – Neuropeptide Y; *AgRP* – Agouti-related
 58 peptide; *MCH* – Melanin concentrating hormone; *CRH* - Corticotropin Releasing Hormone; *TRH* - Thyrotropin
 59 Releasing Hormone; *CART* - Cocaine- and amphetamine-regulated transcript; *POMC* – pro-opiomelanocortin; *CasC3*
 60 - Cancer susceptibility candidate 3; *ZO-1* – zonula occludens-1; *OCCLU* – occludin ; *MUC2* – mucin 2; *MUC13* –
 61 mucin 13

62

63 MATERIALS AND METHODS

64 Study Design

65 Fecal pellets from control and ATB-treated mice were collected at four time points
 66 throughout the experiment to assess microbiome dynamics. Samples were collected at
 67 baseline, post-antibiotic treatment, post-acclimation, and at study termination. Analysis
 68 focused on shifts in alpha and beta diversity, compositional changes at the phylum
 69 level, and dispersion metrics between treatment groups.

70

71 Data Acquisition

72 Raw sequencing data were obtained from the Sequence Read Archive (SRA) under
73 BioProject accession **PREJEB70936**, corresponding to the study by Roubalova et al.
74 (2024), which investigated the gut microbiome's role in appetite regulation in mouse
75 models of anorexia nervosa. Metadata associated with this project were downloaded
76 using the *cyoa* toolkit on the UMD bioi605 cluster. The accession metadata CSV file
77 was parsed and used to link sequence files to experimental conditions.

78 To obtain the data, we first configured the computing environment using the following
79 commands:

- 80 • module add sra
81 • vdb-config –interactive
82 • module add perl
83 • module and cyoa
84 • cyoa –method srownload –input PREJEB70936

85

86

87 The Mus Musculus reference genome (GReM38), annotated by Ensembl was
88 downloaded from [here](#) and is intended to be used for differential expression analysis
89 of the above listed neuropeptides across the three experiment groups.

90

91 **Metadata Processing**

92 The project's metadata (PRJEB70936_sra.csv) was downloaded from NCBI and
93 imported into R, and processed using the *readr*, *dplyr*, and *stringr* packages. Key
94 variables, including mouse identifiers, treatment condition - *control* (CTRL) and *anti-*
95 *biotic treatment* (ATB), and experimental time points were extracted from the protocol
96 field. Cleaned metadata were saved in *mouse_label_data.csv* and linked to FASTQ files
97 for downstream analysis.

98

99 **Quality Control and Trimming**

100 Raw paired-end FASTQ reads were assessed using the *plotQualityProfile()* function in
101 the *DADA2* package. Based on quality score visualization and reference scripts from the
102 study [3], truncation lengths of 270 bp for forward reads and 190 bp for reverse reads
103 were selected. Reads were then trimmed and filtered using the *filterAndTrim()* function
104 with default parameters, removing low-quality bases and reads with ambiguous
105 nucleotides.

106

107 **Denoising, Merging, and Chimera Removal**

108 Filtered reads were dereplicated and denoised using the *dada()* function with
109 *selfConsist=TRUE* to allow joint estimation of error profiles and sample composition.
110 Paired reads were then merged using *mergePairs()*, and amplicon sequence variants
111 (ASVs) were compiled into a count matrix using *makeSequenceTable()*. Chimeric
112 sequences were identified and removed using the *removeBimeraDenovo()* function in
113 DADA2 using the *consensus* method. The resulting non-chimeric ASV table
114 represented high-confidence biological variants across all samples.

115

116 **Taxonomic Assignment and Phyloseq Object Construction**

117 Amplicon sequence variants (ASVs) were classified taxonomically using the
118 *assignTaxonomy()* function in the DADA2 package, with the SILVA v138.2 reference
119 database and a minimum bootstrap confidence of 80. The resulting ASV table,
120 taxonomic assignments, and haplotype sequences (haplo.fasta) were merged into a
121 unified *phyloseq* object. Sample metadata were formatted and added using
122 *sample_data()* to enable grouping by treatment condition and time point.

123

124 **Normalization and Rarefaction**

125 To prepare for diversity analysis, two normalization approaches were applied. First, the
126 dataset was converted to relative abundances using *transform_sample_counts()* in
127 *phyloseq*. Second, to control for uneven sequencing depth across samples, rarefaction
128 was performed using *rarefy_even_depth()* with a fixed random seed for reproducibility.

129

130 **Taxonomic Composition Visualization**

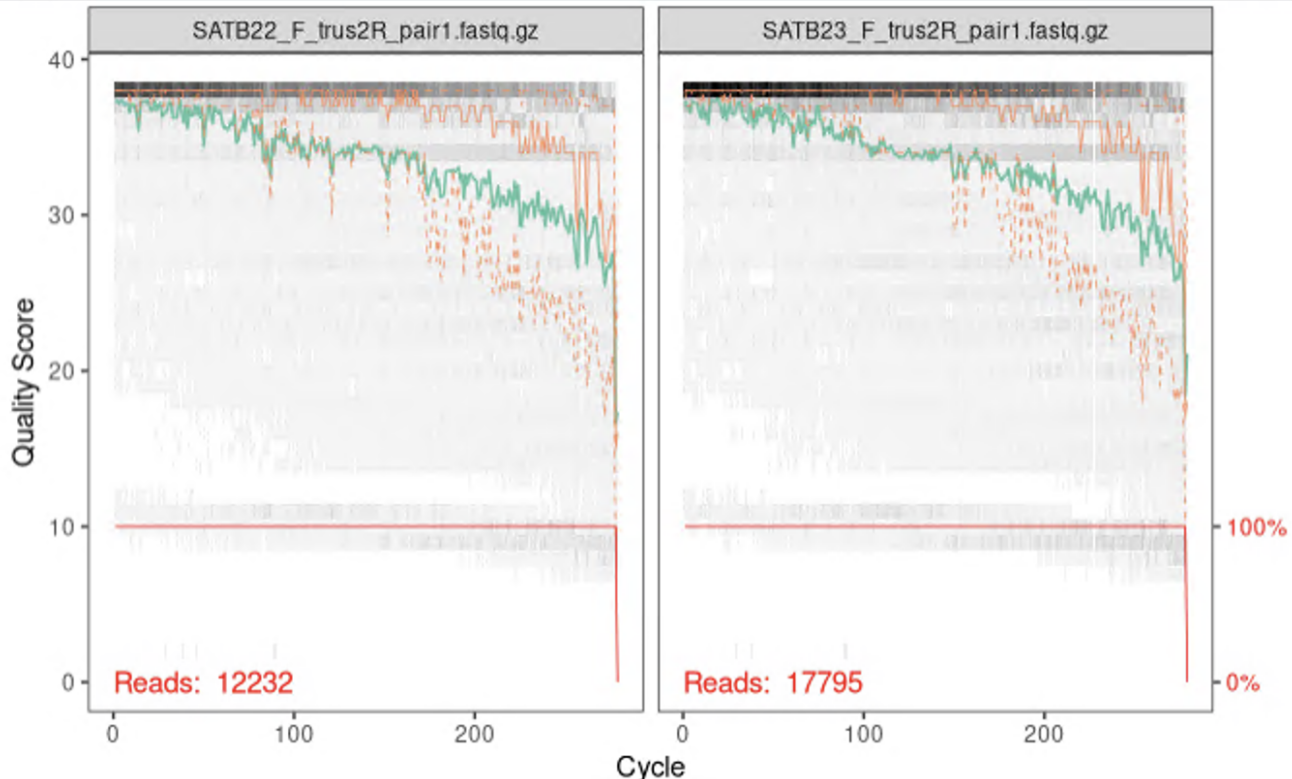
131 Relative abundance data were aggregated at the phylum level using *tax_grom()* and
132 transformed to long format using *psmelt()*. To focus on dominant taxa, only the top eight
133 phyla by total abundance were retained; all others were grouped as "Other." The
134 resulting data were used to generate stacked barplots, grouped by mouse and
135 timepoint, using *ggplot2*.

136

137 **RESULTS**

138 **Visualizing The Quality**

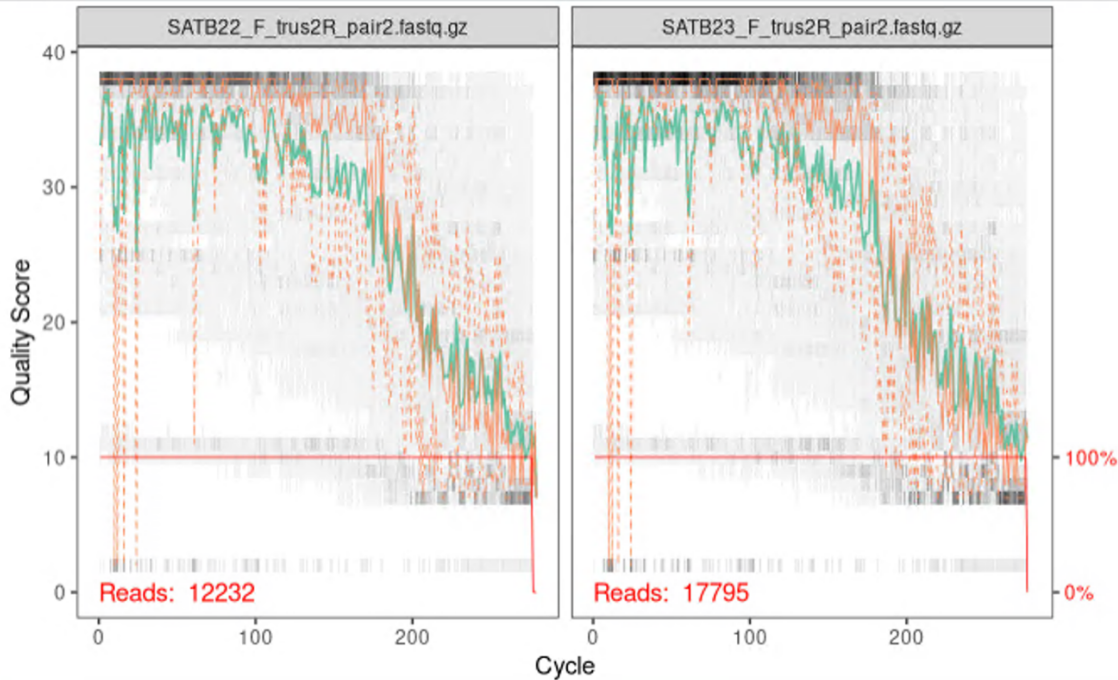
139 Examining the forward read quality plots, we observed that the scores remain high and
140 stable up to approximately cycle 240–250, after which the read quality began to decline.
141 The quality scores for the forward read of two samples, SATB22_F_trus2R and
142 SATB23_F_trus2R are shown in Figure 1 below.



143

144 *Figure 1.* Forward read quality plot

145 The reverse read quality starts to decline after cycle 180. The quality scores for the
146 reverse read of two samples, SATB22_F_trus2R and SATB23_F_trus2R are shown in
147 the plot below (*Figure 2*).

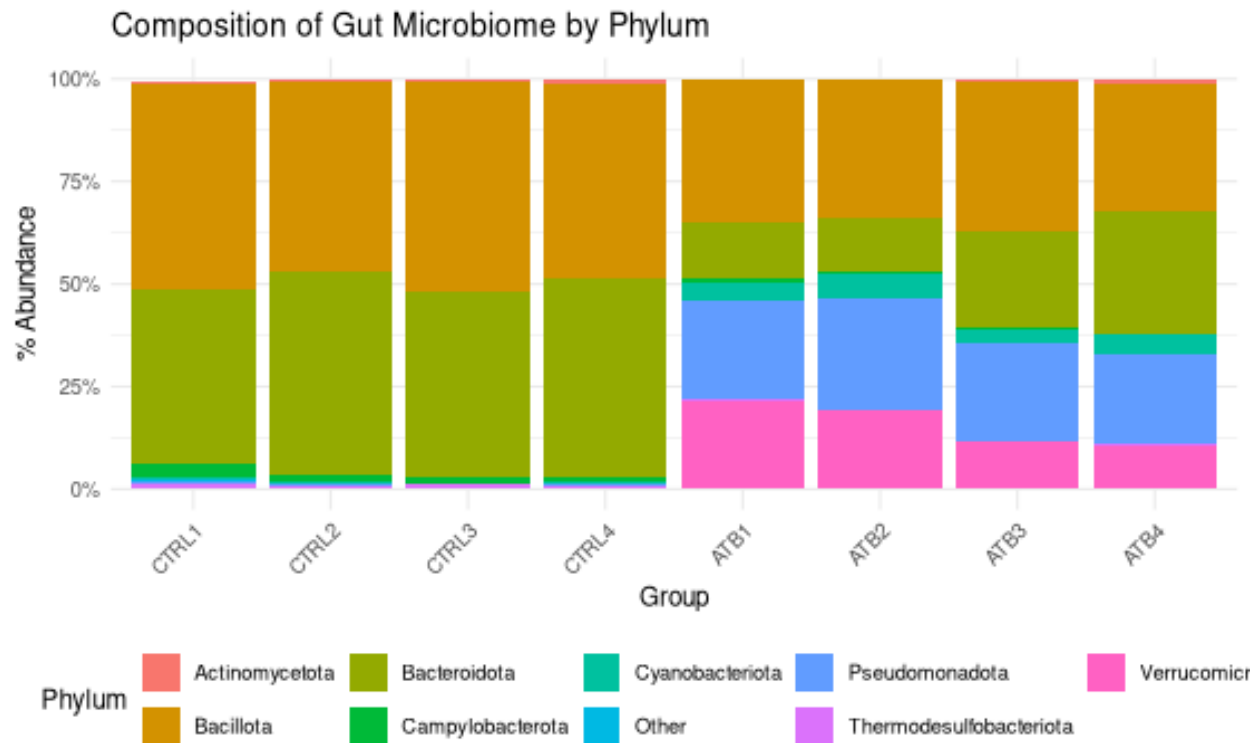


148

149 *Figure 2. Reverse read quality plot*

150 **Taxonomic Composition Bar plot**

151 We investigated the differences in microbial composition across the ATB and CTRL
 152 groups and found that antibiotic exposure disrupted the normal microbial balance
 153 (*Figure 3*). Several bacterial phyla that were nearly absent in the CTRL groups, such as
 154 Pseudomonadota (blue) and Verrucomicrobiota (pink), appeared in the ATB group.



155
156 *Figure 3.* Taxonomic Compositon boxplot, which looks at the average gut microbiome composition (at the phylum
157 level) for a specific group of mice

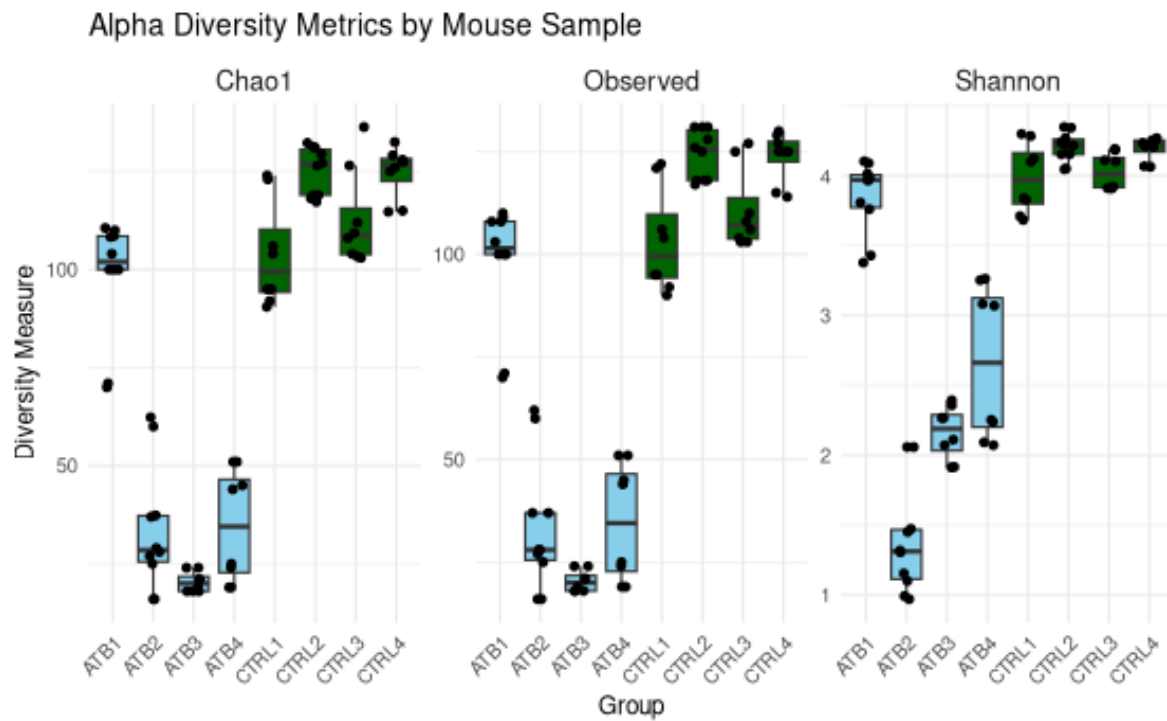
158

159 Alpha Diversity Boxplot

160 To assess within-sample microbial diversity, we calculated three alpha diversity metrics:
161 **Chao1**, **Observed ASVs**, and **Shannon index**. These metrics reflect species richness
162 and evenness across experimental groups. The resulting boxplots (*Figure 4*) revealed
163 that gut microbial alpha diversity was significantly reduced in mice treated with
164 antibiotics (ATB1–ATB4) compared to control groups (CTRL1–CTRL4).

- 165 • Both **Chao1** (*Figure 4a*) and **Observed ASVs** (*Figure 4b*) showed a clear
166 reduction in richness following antibiotic treatment.
- 167 • **Shannon diversity** (*Figure 4c*), which reflects both richness and evenness,
168 declined particularly in the ATB2 and ATB3 groups, indicating substantial
169 disruption to the microbial ecosystem.
- 170 • Notably, **ATB1**, representing the earliest post-treatment timepoint, displayed
171 diversity levels like control mice, suggesting the antibiotics had not yet taken
172 effect.
- 173 • By **ATB4**, a slight increase in all three metrics was observed, indicating partial
174 recovery of the gut microbiome.

175 These patterns underscore the temporal impact of antibiotic exposure on microbial
176 communities and support the use of these metrics as sensitive indicators of gut
177 dysbiosis and recovery.



178

179 *Figure 4.* Visualization of the alpha diversity metrics. Chao1 box plot (a) estimated total richness including rare taxa.
180 Observed box plot (b) the count of the unique taxa. Shannon box plot (c) richness and evenness how evenly taxa are
181 distributed.

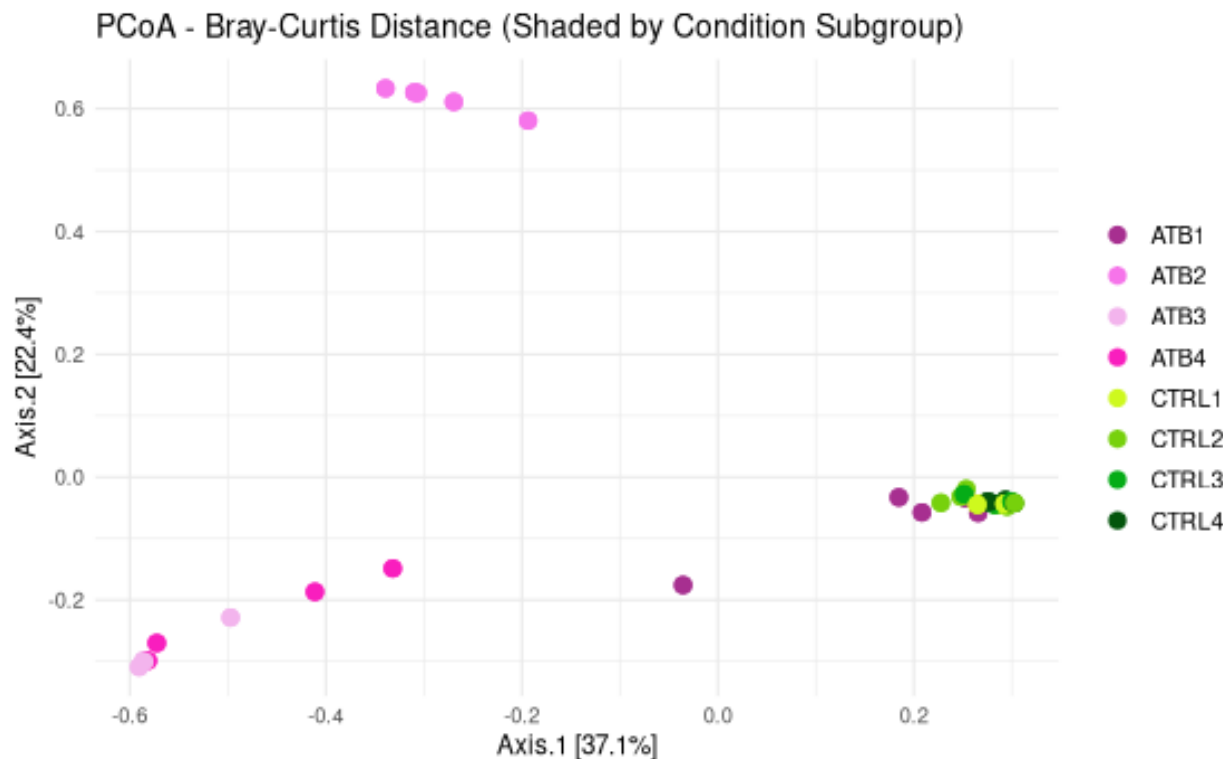
182

183 Beta Diversity Plot

184 To assess between-sample differences in gut microbiome composition, a Principal
185 Coordinates Analysis (PCoA) was performed using Bray-Curtis distance metrics. Each
186 point in the ordination plot represents the microbial community of an individual mouse at
187 a specific timepoint (*Figure 5*). The first principal coordinate (Axis 1) accounts for 37.1%
188 of the total variation, while the second principal coordinate (Axis 2) explains 22.4%.

189 Control (CTRL) mice clustered closely together, indicating a high degree of similarity in
190 their microbiome composition over time. In contrast, antibiotic-treated (ATB) mice were
191 more widely dispersed and formed distinct clusters separate from the CTRL group,
192 suggesting that antibiotic exposure created a significant impact on microbial community
193 structure. Likewise, ATB1 samples clustered nearer to the CTRL group, reflecting their

194 collection before antibiotic administration. These results highlight the substantial impact
195 of antibiotic treatment on microbiome composition and its progression over time.



201 This analysis highlights the profound and dynamic effects of antibiotic treatment on the
202 gut microbiome in a mouse model relevant to anorexia nervosa. Across all three-
203 diversity metrics—Observed ASVs, Chao1, and Shannon index—mice exposed to
204 antibiotics exhibited reduced microbial richness and evenness, particularly at midpoints
205 (ATB2 and ATB3). Beta diversity analysis further revealed that antibiotic-treated mice
206 developed distinct microbial communities, diverging significantly from the stable
207 samples observed in control groups. These findings suggest that antibiotic exposure
208 induces acute dysbiosis, but may allow for partial recovery over time, as evidenced by
209 increased diversity metrics in ATB4.

210

211 The emergence of phyla such as *Pseudomonadota* and *Verrucomicrobiota* in antibiotic-
212 treated groups underscores a compositional shift that may be linked to altered host-
213 microbiota interactions. Furthermore, the ATB-treated mice were seen to have
214 significantly reduced percentage abundance of Bacteroidota and Bacillota, which make

215 up much of the gut microbiome composition in the control groups. Lower levels of
216 Bacteroidota have been linked with chronic gut inflammation – specifically with
217 Inflammatory Bowel Disease [4].

218 With the gut microbiome's role in modulating neuropeptides related to appetite and
219 behavior, these microbial shifts may have downstream implications for hypothalamic
220 signaling and metabolic regulation.

221

222 **LIMITATIONS**

223 A limitation to our analysis was that the neuropeptide expression levels in the
224 hypothalamus were assessed using quantitative PCR (qPCR) rather than
225 transcriptome-wide RNA-sequencing (RNA-seq). Without raw sequencing data, we
226 could not perform gene level quantification and investigate gene expression levels for
227 the specific neuropeptides originally targeted in the paper, and our study was limited to
228 studying microbiome composition differences across different experimental groups.

229

230

231

232

233

234

235

236

237

238

239

240

241

242

243

244

245 **BIBLIOGRAPHY**

- 246 1. Roubalová R, Procházková P, Kovářová T, Ježková J, Hrnčíř T, Tlaskalová-
247 Hogenová H, Papežová H. 2024. Influence of the gut microbiome on appetite-
248 regulating neuropeptides in the hypothalamus: Insight from conventional, antibiotic-
249 treated, and germ-free mouse models of anorexia nervosa. *Neurobiology of Disease*
250 **193**: 106460.
- 251 2. Roubalová R, Procházková P, Papežová H, Smitka K, Bilej M, Tlaskalová-
252 Hogenová H. 2020. Anorexia nervosa: Gut microbiota-immune-brain interactions.
253 *Clin Nutr* **39**: 676–684.
- 254 3. JanetJezkova. 2023. JanetJezkova/Gut-microbiota_ABA-model_2023.
255 https://github.com/JanetJezkova/Gut-microbiota_ABA-model_2023 (Accessed May
256 13, 2025).
- 257 4. Zhou Y, Zhi F. Lower Level of Bacteroides in the Gut Microbiota Is Associated with
258 Inflammatory Bowel Disease: A Meta-Analysis. *BioMed Res Int.* 2016;2016:
259 5828959. doi:10.1155/2016/5828959

260